Adjoint Electron-Photon Transport Monte Carlo Calculations with ITS

Leonard J. Lorence, Ronald P. Kensek, John A. Halbleib
Sandia National Laboratories
Albuquerque, NM 87185-1179

J. E. Morel
Los Alamos National Laboratory
Los Alamos, NM 87545

ABSTRACT

A general adjoint coupled electron-photon Monte Carlo code for solving the Boltzmann-Fokker-Planck equation has recently been created. It is a modified version of ITS 3.0, a coupled electron-photon Monte Carlo code that has world-wide distribution. The applicability of the new code to radiation-interaction problems of the type found in space environments is demonstrated.

I. INTRODUCTION

In conventional or forward radiation transport one effectively calculates a desired response λ as an inner product of the particle flux ψ and the response function R:

$$\lambda = (\psi, R) \tag{1}$$

The inner product spans the phase space of the problem under consideration. Particles are transported in phase space, which most generally consists of seven coordinates: time, energy, two angular coordinates and three spatial coordinates. In the absence of biasing[1], ψ will span a large region of the phase space. This is of little consequence, and indeed can be beneficial, when the response function also spans a large region of phase space; e.g., many dose detectors over the entire application geometry. For a response function that is highly restricted in phase space, however, (e.g., a small collimated detector of a narrow band of particle energies inside a complex satellite geometry), forward transport can be very inefficient. Moreover, this inefficiency will be compounded if results for an ensemble of sources that also spans a large region of phase space are needed. In this case multiple calculations will be required.

It turns out that in just those situations for which Eq. (1) is most inefficient, an alternative method for calculating λ is most efficient:

$$\lambda = (\psi^\dagger, Q) \tag{2}$$

In this method one solves the adjoint transport equation for the adjoint flux $\psi^\dagger$ using an adjoint source $Q^\dagger$ derived from the response function. The inner product of the adjoint flux with a source Q yields the desired response. Because the adjoint flux will also generally span a broad range of phase space, a single adjoint calculation will yield λ for a broad range of sources. More specifically, results can be obtained as a function of the phase-space parameters of the source. Thus, while conventional forward transport is most efficient when the phase space of the source is restricted and the phase space of the response is broad, adjoint transport will be most efficient when the opposite is true. For the great majority of applications that fall in between these extremes, the choice between forward and adjoint will not be so obvious and will depend on such considerations as the biasing capability of the available software in both forward and adjoint mode as well as the ingenuity of the analyst.

It is clear from the above considerations that the adjoint method can be ideally suited to the simulation of localized detector responses in satellites and other space vehicles to space-radiation environments. Space-radiation sources are already broadly distributed in energy and angle, and mission-averaged sources will also be broadly distributed over the outer surfaces of these vehicles. Moreover, the method can be equally useful when the responses to an ensemble of sources, or equivalently the responses as a function of phase space parameters, are required.

In this paper we discuss the application of a new code system for coupled electron/photon transport, the Multigroup/Continuous-Energy (hybrid) Integrated TIGER Series (MITS) Monte Carlo code system, that has a capability for three-dimensional adjoint transport. It is a version of the Integrated TIGER Series (ITS 3.0)[2], a powerful and user-friendly system of coupled electron/photon Monte Carlo transport codes that can be employed to simulate accurate responses to electron and photon sources. The ACCEPT code of the ITS system permits these simulations to be carried out in complex three-dimensional geometries. However, the ITS codes are continuous-energy codes, and implementation of the adjoint method in such codes is generally quite difficult [3]. Consequently, the

0018-9499/95$04.00

ITS system has no adjoint capability. The CEPXS/ONELD code system[4], on the other hand, provides a very fast and accurate solution for one-dimensional electron/photon transport applications using the method of discrete ordinates. Because it is a multigroup-energy code, it can perform adjoint transport as well as forward transport. However, because of memory constraints and limited geometric modeling algorithms, robust three dimensional deterministic codes are not yet available for electron transport. The MITS code system was developed to provide a flexible three-dimensional adjoint capability that is lacking in either the ITS or CEPXS/ONELD code systems.

The MITS system combines the cross-section generator from CEPXS/ONELD and the input/output and combinatorial geometry routines from ITS to obtain the Monte Carlo solution of the time-independent Boltzmann-Fokker-Planck (BFP) equation[5]. The forward form of the BFP equation is:

$$\vec{\Omega}\cdot\vec{\nabla}\psi + \sigma_t(\vec{r},E)\,\psi = Q(\vec{r},E,\vec{\Omega}) + \tag{3}$$

$$\int_0^\infty dE' \int_0^{4\pi} d\vec{\Omega}'\,\sigma_s(\vec{r},E'\to E,\vec{\Omega}'\to\vec{\Omega})\,\psi(\vec{r},E',\vec{\Omega}')$$

$$+\frac{\alpha(\vec{r},E)}{2}\left(\frac{\partial}{\partial\mu}\left[(1-\mu^2)\frac{\partial\psi}{\partial\mu}\right]+\frac{1}{1-\mu^2}\frac{d^2\psi}{d\phi^2}\right)$$

$$+\frac{\partial}{\partial E}[S(\vec{r},E)\,\psi]$$

and the adjoint BFP equation is:

$$-\vec{\Omega}\cdot\vec{\nabla}\psi^\dagger + \sigma_t(\vec{r},E)\,\psi^\dagger = Q^\dagger(\vec{r},E,\vec{\Omega}) + \tag{4}$$

$$\int_0^\infty dE' \int_0^{4\pi} d\vec{\Omega}'\,\sigma_s(\vec{r},E\to E',\vec{\Omega}\to\vec{\Omega}')\,\psi^\dagger(\vec{r},E',\vec{\Omega}')$$

$$+\frac{\alpha(\vec{r},E)}{2}\left(\frac{\partial}{\partial\mu}\left[(1-\mu^2)\frac{\partial}{\partial\mu}\psi^\dagger\right]+\frac{1}{1-\mu^2}\frac{d^2}{d\phi^2}\psi^\dagger\right)$$

$$-\frac{\partial}{\partial E}[S(\vec{r},E)\,\psi^\dagger] + \left(\frac{\partial}{\partial E}S(\vec{r},E)\right)\psi^\dagger$$

In these equations, ϕ and μ are the two angular coordinates, which can also be represented by the vector, $\vec{\Omega}$, and $\vec{r}$ represents the three spatial coordinates.

In each equation, the first two lines contain the Boltzmann terms and the sources, Q and $Q^\dagger$. The subsequent lines contain the Fokker-Planck terms. The material-dependent total cross section, σ_t, and the transfer cross section, σ_s appear in the Boltzmann part of the equation. These cross sections represent all photon interactions and a subset of electron interactions. Those electron interactions that result in small-angular deflections or small-energy losses are represented by the Fokker-Planck terms, rather than by a cross section. The material-dependent quantities in these terms represent the aggregate of many interactions. They include α, the restricted momentum transfer[6] and S, the restricted stopping power[7].

The CEPXS code[7] assembles the cross section data in multigroup-Legendre format. Like other multigroup Monte Carlo codes[8], MITS converts these data into cumulative probability distributions that represent the center-of-mass scattering from angle to angle for each group-to-group transition in each material. In neutral-particle multigroup codes, particles are not assigned a discrete energy. Rather, the codes only keep track of the particle's group index. In MITS, the proper treatment of the restricted stopping power requires that particles possess a discrete energy in addition to a group index. The discrete energy is needed to properly account for Fokker-Planck energy losses, and the group index is used to properly account for Boltzmann scattering events. Hence, MITS is a hybrid continuous-energy/multigroup code. In this regard, it resembles NOVICE[9], the first electron Monte Carlo code to be developed with an adjoint capability. MITS makes use of a new algorithm for the solution of the BFP equation developed by Morel et al.[10], a preliminarily version of which was tested in MCNP[11]. The BFP equations solved by MITS are fully coupled in that electrons can generate photons and photons can generate electrons. As will be shown, MITS can be used for shielding calculations with electron sources as well as photoemission calculations with X-ray sources.

II. Experimental and Theoretical Benchmarks in One-Dimensional Slab Geometry

Currently, the MITS code system consists of a one-dimensional code that has the slab geometry of TIGER and a general three-dimensional code that has the combinatorial geometry of ACCEPT. For many benchmarks to experimental data, it is sufficient to use the slab geometry version of MITS. Lockwood et al. [12] measured the dose profile in an aluminum/gold/aluminum multilayer configuration for a normally incident 1.0-MeV beam of electrons. The front aluminum layer (nearest the source) is 0.017-cm-thick, the gold layer is 0.0022-cm-thick, and the back aluminum layer is 0.152-cm-thick.

In Figure 1, the dose profile from a forward MITS calculation is compared to experiment and to an ITS-3.0 solution. Good agreement is obtained. In the MITS calculation, fifty logarithmic groups were used both for the electrons and the photons, respectively, and the cutoff energy was chosen to be 0.01 MeV for both. Fifty thousand histories were used in both Monte Carlo calculations, and the run times were comparable (about 1800 seconds on an IBM 560 workstation).

While one forward calculation is sufficient to obtain the dose profile of Figure 1, many adjoint transport calculations would be required to assemble the same profile. This is because a different adjoint source $Q^{\dagger}$ would be needed for each spatial interval of the profile.

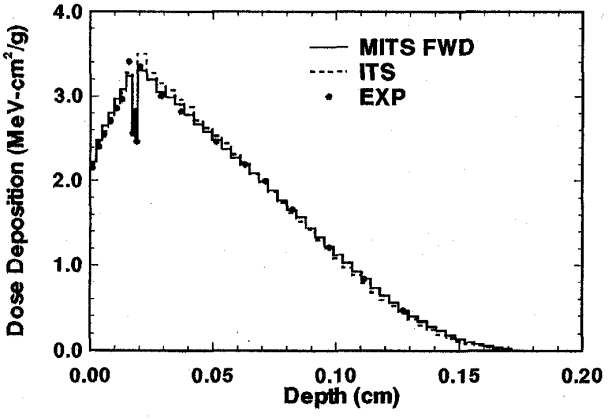

FIGURE 1. Dose profile due to a normally-incident 1.0-MeV electron source incident on an Al/Au/Al slab - comparison of MITS in forward mode with ITS and experiment

We performed adjoint transport calculations to obtain the dose in some of the spatial intervals of Figure 1. These predictions are compared to those obtained with MITS in forward transport mode in Figure 2. In order to expedite the adjoint transport, the source, Q, was represented as an isotropic angular flux distribution over 0-20° with respect to the target normal. Excellent agreement between the forward and the adjoint transport solutions of MITS was obtained.

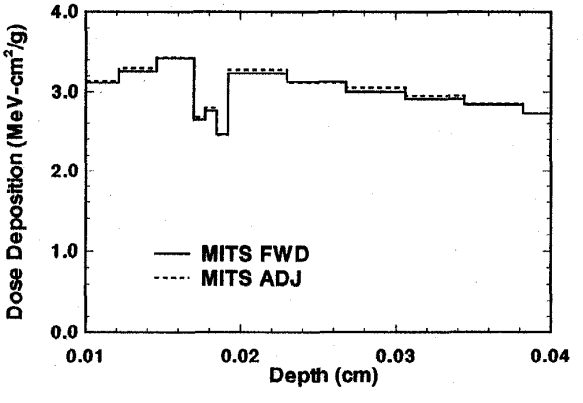

FIGURE 2. Dose profile due to a 1.0-MeV electron source with an isotropic angular flux distribution from 0-20° incident on an Al/Au/Al slab - comparison of MITS in forward mode with MITS in adjoint mode.

Lockwood et al. [13] also measured the albedos for electrons incident on various materials that are thick to the range of the electrons. These experiments are well-suited for modelling in adjoint mode since the electron albedos were measured for an ensemble of sources varying in energy and angle. In Figure 3, the albedos for aluminum obtained from a single MITS adjoint solution are compared to the experimental data and to a discrete ordinates (DO) adjoint calculation obtained with the CEPXS/ONELD code. Two curves are shown, one for an experimental data set in which the electron sources are normally incident and the other for a set of sources incident at an angle of 60°. Good agreement between the codes and the data is obtained.

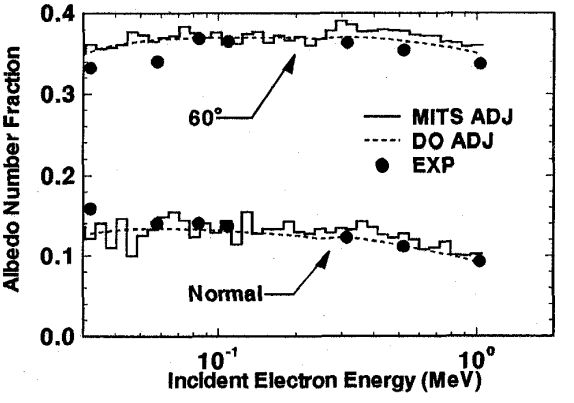

FIGURE 3. Electron albedos due to mono-energetic electron sources incident on an aluminum slab - comparison of MITS in adjoint mode with adjoint DO and experiment.

A cutoff energy of 0.01 MeV was used in both predictions. The adjoint MITS calculation was performed with fifty logarithmic groups for both electrons and photons, respectively. With four million particle histories, the Monte Carlo calculation took 9400 seconds on the IBM workstation. In the adjoint MITS prediction, an isotropic angular flux from 0-10° with respect to the target normal was used to model the data set at normal incidence, and an isotropic angular flux over the angular interval from 50-70° was used to model the other data set. The DO adjoint predictions were interpolated to 0° and 60°.

Experimental benchmarks also exist for photoemission. The data of Grudskii et al. [14] has been previously used to benchmark DO codes [15]. In Figures 4 and 5 the total photoemission yield from foils of tantalum and gold, respectively, are calculated for mono-energetic, normally incident photon x-rays. The gold foil was 0.000337-cm thick and two thicknesses of tantalum were used, a 0.0102-cm foil at the lower energies and a 0.039-cm foil at the higher energies. Since separate adjoint predictions are required for each material thickness, two adjoint photoemission curves for tantalum are presented in Figure 4. The MITS adjoint solutions agree well with DO solutions and with experiment.

In the Monte Carlo calculations, fifty logarithmic groups were used for both electrons and photons, respectively. In the

gold transport calculation and the lower-energy tantalum calculation, the cutoff energy was set to 0.001 MeV. For the adjoint predictions at the higher energies in tantalum, the cutoff energy was set to 0.03 MeV. Also, at the higher energies in tantalum, pair secondary production was included in the particle transport model in both Monte Carlo and DO, and the pair secondaries were counted in the photoemission yield. However, the positrons were tracked as electrons. Four million histories were used for the gold and lower-energy tantalum Monte Carlo predictions. The run times for these calculations consumed about 25000 seconds on the IBM workstation. Ten million histories were employed for the higher-energy adjoint Monte Carlo solution and the run time scaled accordingly.

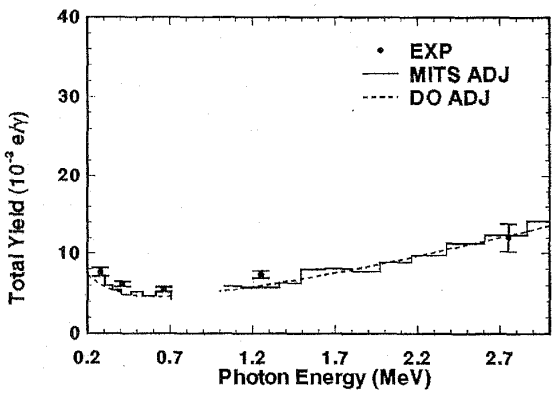

FIGURE 4. Total photoemission yield due to monoenergetic x-ray sources normally incident on tantalum foils - comparison of MITS in adjoint mode with adjoint DO and experiment.

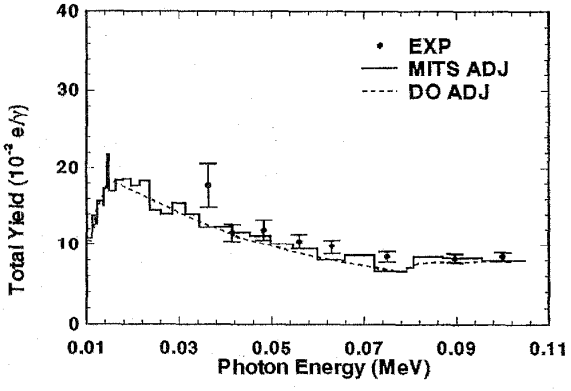

FIGURE 5. Total photoemission yield due to monoenergetic x-ray sources normally incident on a gold foil - comparison of MITS in adjoint mode with adjoint DO and experiment.

III. ADJOINT CALCULATIONS WITH THE THREE-DIMENSIONAL MITS CODE

Saqui et al.[16] have developed a set of computational benchmarks to investigate calculational methodologies used in satellite shielding and survivability applications. To demonstrate the utility of the MITS code system for three-dimensional problems of interest to the space-environment community, we have selected a few of these benchmarks for comparisons.

All of these benchmarks consist of very simple geometries. There are fifteen different configurations, each with from one to four specified points at which dose is to be calculated. The source is omnidirectional (isotropic flux), normalized to one free-space electron per square centimeter, which corresponds to a surface (current) source of 0.25 electrons per square centimeter over all non-convex external surfaces with a 2π cosine-law angular distribution with respect to the inward normal. There are four specified source-energy distributions, two of which are mono-energetic.

We examined two benchmark geometries from this set that were not possible to represent with a slab-geometry transport code. The first benchmark geometry is a solid aluminum sphere. Because of symmetry of the source and material geometry, this benchmark can be modelled as a one-dimensional problem in spherical coordinates. However, since a one-dimensional spherical-geometry code is not included in either MITS or ITS, the Monte Carlo results were actually obtained with three-dimensional codes. Results were also obtained with the CEPXS/ONELD code. For this case, the DO code was run in forward-transport mode in one-dimensional spherical geometry. Later in this section, we will introduce a second benchmark geometry that is strictly three-dimensional.

As shown in Figure 6, there are two dose points specified for this benchmark problem. The first is at the center of the 0.5-cm radius sphere, the second is at a radius of 0.35 cm.

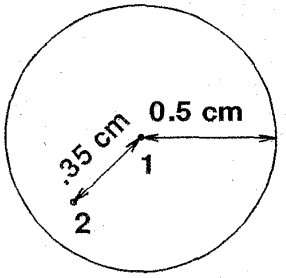

FIGURE 6. Geometry for the solid aluminum sphere benchmark. Dose is calculated at the center (Dose Point 1) and at a radius of 0.35 cm (Dose Point 2).

Since it is not possible to calculate dose at a point with a forward Monte Carlo code (either ITS or MITS), a finite-sized

volume must be specified. For the forward Monte Carlo calculations only, Dose Point 1 was represented by a sphere of radius 0.05 cm and Dose Point 2 was represented by a spherical shell between radii 0.345 cm and 0.355 cm.

We will first consider the highest mono-energetic source energy of 5 MeV. Since ITS is a forward continuous-energy code, there is no problem in describing such a source. In MITS, particles also carry a continuous energy, but the default at present for the forward mode is to sample source particles with energies uniformly distributed within the group containing the mono-energetic source energy. For 50 logarithmic groups starting with one centered at 5 MeV and extending down to .001 MeV, this results in a source of 5 MeV ± 8.6%. The results show no dependence on the finite-energy spread of this representation of the source. The same group structure is used in the adjoint-MITS calculations. For ITS, the electron cutoff is 5% of the source energy. The cutoff energy for photons is 0.01 MeV. For MITS, both the electron and photon cutoffs are 0.001 MeV, respectively, which are the present default cutoffs for the group structure.

The results are shown in Figure 7, normalized by the ITS-3.0 calculation. For the Monte Carlo calculations, error bars representing one-sigma estimated uncertainties are also shown. To facilitate comparison between the forward and adjoint, the dose was most often determined in Rads(Al) (the resident material). As can be seen, the agreement among all the codes is excellent. The adjoint MITS calculation was also calculated in Rads(Si) to facilitate comparison with the Novice code. The dose in Rads(Si) is seen to be slightly higher than the dose in Rads(Al).

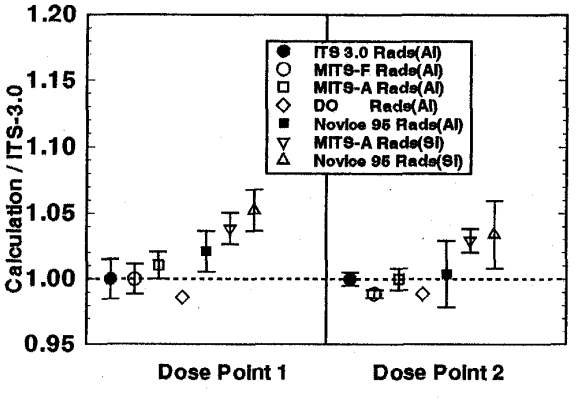

FIGURE 7. Results of dose calculations for a 5-MeV mono-energetic electron source for the solid sphere.

Note: Novice has undergone incremental improvements since the benchmark report[16], so the results shown in Figure 7 (as "Novice 95") have been obtained[17] with the current version of the code. One significant change to Novice is the inclusion of improved bremsstrahlung production data. Use of the current version of Novice has resulted in better agreement with the other codes.

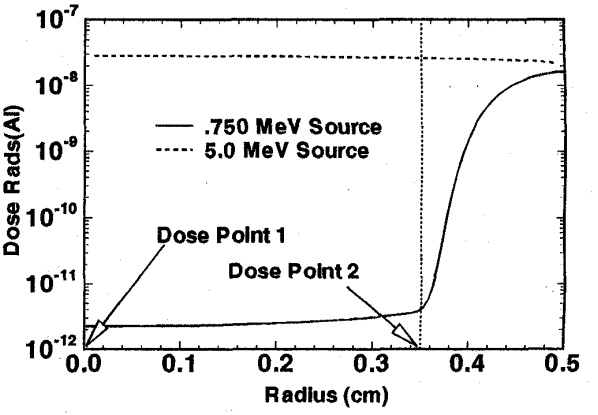

FIGURE 8. Radial dose profiles for the solid aluminum sphere benchmark obtained with DO. The dose profile for the .750-MeV source is difficult to calculate with Monte Carlo.

Figure 8 shows the radial dose deposition as calculated by the DO code (which was used only because it was much easier to get finer radial resolutions than with Monte Carlo). For the 5-MeV source, the 0.5-cm sphere is rather thin to the electrons, the dose is dominated throughout by the primaries, and the profile is quite flat. The DO calculation indicates that the point dose decreases by less than 1% in moving out to a radius of 0.05 cm from the center, so no significant error was accrued with the finite volumes.

The situation is quite different for the lowest mono-energetic electron source specified in the benchmark calculation set (0.750 MeV), also shown in Figure 8. Dose Point 1 sits on the bremsstrahlung tail, far beyond the range of the primaries. Dose Point 2 is at the end of the range of the source particles where the calculated dose will be very sensitive to straggling. Doses at both of these points are quite challenging to calculate with Monte Carlo.

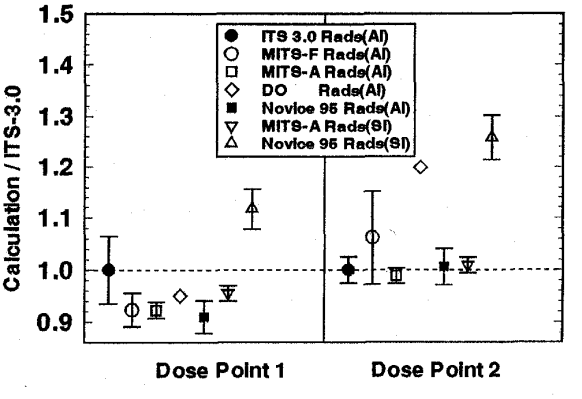

FIGURE 9. Results of dose calculations for a 0.75-MeV mono-energetic electron source for the solid sphere.

Based on our experience with ITS, we have built into the MITS code system some of the major components of a general biasing scheme[18] to help solve such "combined x-ray effects" problems where the dose due to the radiation of an electron beam is needed. These components include spatially-dependent scaling of the cross sections to help convert one particle species to another (e.g., electrons to photons via bremsstrahlung and impact ionization), Russian Roulette kill of secondary electrons (e.g., Compton and photo-electrons that have low probabilities of contributing to the desired response), and photon forcing. All of the MITS calculations for the 0.750-MeV source shown in Figure 9 made use of some of these features.

The strategy was similar for the forward and adjoint MITS calculations (both using 50 logarithmic groups from 0.75 MeV to 0.001 MeV). For example, in the forward calculation to calculate dose at the center, the source electrons were converted to photons as quickly as possible by scaling up the bremsstrahlung cross sections while performing Russian Roulette on photon-produced electrons. These photons were transported and forced to interact in the dose region near the center where Russian Roulette was ignored.

The ITS run in Figure 9 was unbiased for comparison purposes. Despite a much longer run time (25.7 hours - ITS vs. 7.5 hours - MITS), it was necessary to expand the dose deposition zone from 0.05 cm to 0.1 cm to keep the estimated statistical uncertainties reasonable. From the radial dose profiles shown in Figure 8, it can be expected that the ITS calculation would thereby be high by about 1.5%. The agreement shown in Figure 9 among ITS, MITS and Novice for Rads(Al) is excellent. This paper does not attempt to resolve any differences with the Novice calculations for Rads(Si).

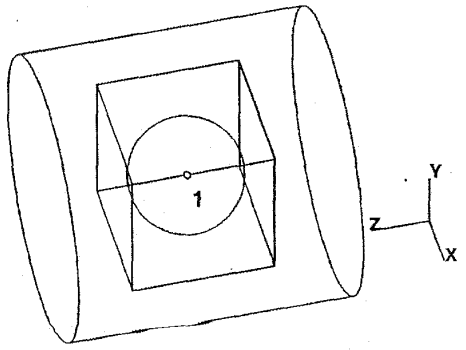

FIGURE 10. Geometry for mixed benchmark. The single dose point is in the center of the solid aluminum sphere.

The geometries in the computational benchmark set[16] get no more complicated than the mix shown in Figure 10. This benchmark geometry consists of three concentric bodies: a sphere, a cube and a cylinder. The inner solid aluminum sphere has a radius 0.2 cm, the surrounding otherwise-empty cube has an edge length of 0.5 cm, and the surrounding otherwise-aluminum cylinder has a length and a diameter of 1 cm. The cylinder axis is parallel to four edges of the cube. The only specified dose point is in the center of the nested solid aluminum sphere.

The results (all unbiased) for the 5-MeV mono-energetic electron source are shown in Figure 11. The cutoffs, group structure, and size (0.05 cm) of the deposition zone used for the forward calculations are the same as those used for Dose Point 1 for the solid sphere (Figure 6) with the 5-MeV source. The agreement for Rads(Al) is excellent: note the expanded scale. A CEPXS/ONELD discrete ordinates solution was not possible because the problem is no longer one-dimensional.

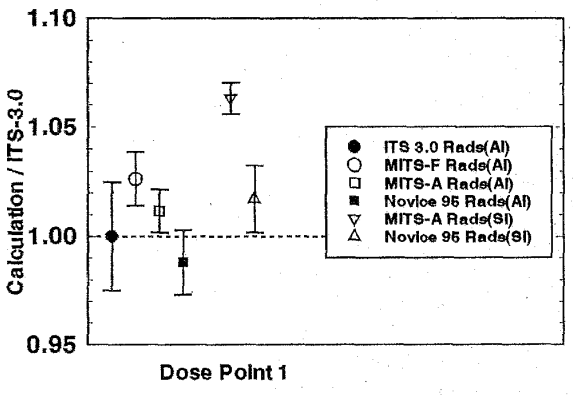

FIGURE 11. Results of dose calculation for a 5 MeV mono-energetic electron source for the mixed geometry.

As previously mentioned, one of the major advantages of an adjoint calculation is improved efficiency, especially for calculations involving a restricted region of phase space such as the point-dose calculations discussed here. For Monte Carlo calculations, it only makes sense to compare run times for results with comparable statistical uncertainties, so we use a figure of merit (FOM) defined as

$$FOM = \frac{t_F \cdot \sigma_F^2}{t_A \cdot \sigma_A^2} \tag{5}$$

where t is the run time and σ^2 is the variance of the forward (F) or adjoint (A) calculation. The FOM represents how much longer it would take to run the forward calculation to get a comparable variance for the two runs. Since no attempt was made to optimize the biasing for the 0.75 MeV source, only results for the 5 MeV source (which were all unbiased) are shown.

Table 1 indicates the adjoint calculations were always much more efficient for these problems. For the sphere, the adjoint calculation for the center dose point is relatively more efficient than the point at 0.35 cm. This is expected since in the forward calculation the center dose region subtends a much smaller solid angle at a source position than the region at a radius of 0.35 cm.

TABLE 1. Figure of Merit indicating improved efficiency of adjoint over forward calculations.

Geometry	Dose Point	FOM
Sphere (Figure 6)	Point 1	75
Sphere (Figure 6)	Point 2	8.2
Mix (Figure 10)	Point 1	25

IV. CONCLUSIONS

An adjoint transport version of the electron-photon Monte Carlo transport code ITS has been created. This new code, MITS, relies on a multigroup-energy approximation and multigroup-Legendre cross sections produced by the CEPXS code. The MITS code has been benchmarked with both experimental data and other transport codes such as ITS and CEPXS/ONELD for dose, electron albedo and photoemission yield. Many biasing options have been incorporated into MITS for both forward and adjoint transport. The utility of the three-dimensional adjoint capability of MITS has been demonstrated for a few theoretical benchmarks. For some deep-shielding problems, the adjoint version of MITS can be much more efficient than conventional or forward Monte Carlo transport and may provide the only practical means of obtaining a solution.

V. ACKNOWLEDGMENT

This work was performed at Sandia National Laboratories supported by the U.S. Department of Energy under contract DE-AC04-94AL8500.

VI. REFERENCES

[1] Richard L. Morin, *Monte Carlo Simultation in the Radiological Sciences*, CRC Press (1988).

[2] J. A. Halbleib, R. P. Kensek, T. A. Mehlhorn, G. D. Valdez, S. M. Seltzer, and M.J. Berger, *ITS: The Integrated TIGER Series of Electron/Photon Codes - Version 3.0*, IEEE Trans. Nucl. Sci., 39, 1025, (1992).

[3] J. A. Halbleib, Sr., *Continuous-Energy Adjoint Monte Carlo Theory of Coupled Continuum/Discrete Radiation Transport*, Nucl. Sci. and Eng., 80, 162 (1982).

[4] L. J. Lorence, Jr., J. E. Morel, G. D. Valdez, *Results Guide to CEPXS/ONELD: A One-Dimensional Coupled Electron-Photon Discrete Ordinates Code Package, Version 1.0*, SAND89-22111, Sandia National Laboratories, (1990).

[5] C. R. Drumm, W. C. Fan, and J. H. Renken, *Forward and Adjoint Methods and Applications for Deterministic Electron-Photon Transport*, Nucl. Sci. and Eng. 108, 16-49 (1991).

[6] M. Landesmann and J. E. Morel, *Angular Fokker-Planck Decomposition Representation Techniques*, Nucl. Sci. and Eng., 103, 1-11 (1989).

[7] L. J. Lorence, Jr., J. E. Morel, G. D. Valdez, *Physics Guide to CEPXS: A Multigroup Coupled Electron-Photon Cross-Section Generating Code*, SAND89-1685, Sandia National Laboratories, (1989).

[8] D. P. Sloan, *A New Multigroup Monte Carlo Scattering Algorithm Suitable for Neutral and Charged-Particle Boltzmann and Fokker-Planck Calculations*, SAND83-7094, Sandia National Laboratories (1983).

[9] T. M. Jordan, *Adjoint Electron Monte Carlo Calculations*, Trans. Am. Nucl. Soc., 52, 382 (1986).

[10]J. E. Morel, L. J. Lorence, R. P. Kensek, J. A. Halbleib, and D. P. Sloan, *A Hybrid Multigroup/Continuous-Energy Monte Carlo Method for Solving the Boltzmann-Fokker-Planck Equation*, submitted to Nucl. Sci. and Eng.

[11]J. Briesmeister, Memorandum X-6:JFB-88-292 on Version 3B of MCNP, Los Alamos National Laboratory (1988).

[12]G. J. Lockwood, L.E. Ruggles, G. H. Miller, and J.A. Halbleib, *Calorimetric Measurement of Electron Energy Deposition in Extended Media - Theory vs. Experiment*, Sandia National Laboratories, SAND79-0414 (1980).

[13]G. J. Lockwood, L.E. Ruggles, G. H. Miller, and J.A. Halbleib, *Electron Energy and Charge Albedo -- Calorimetric Measurement vs. Monte Carlo Theory*, Sandia National Laboratories, SAND80-1968 (1981).

[14]M. Y. Grudskii, N.N. Roldugin, V.V. Dmirnov, A.F. Adadyriv, V.T.Lazurik, *Experimental Investigation and Monte Carlo Calculation of Photon-Induced Electron Emission from Solids*, Nucl. Instr. and Methods in Phy. Res., 227,. 126, (1984).

[15]L. J. Lorence, Jr., *Electron Emission Predictions with CEPXS/ONETRAN*, IEEE Tran.Nucl. Sci., 35 (6), 1288, (1988).

[16]R. Saqui, T. Jordan, J. Mack, G. Radke, J. Morel, and J. Janni, *Computational Benchmarks for Electron Total Dose Shielding Methodology*, Air Force Systems Command Weapons Laboratory, WL-TR-90-59, (1991).

[17]T. Jordan, private communication.

[18]J. A. Halbleib, R. P. Kensek, and G. D. Valdez, *Variance Reduction Unique to Coupled Electron/Photon Monte Carlo Transport*, in Proceedings of *Advanced Monte Carlo Computer Programs for Radiation Transport*, NEA/OECD Saclay, France, 141-153, (April 27-29, 1994), ISBN 92-64-14376-9.